Impedance Characterization of AlGaN/GaN/Si High Electron Mobility Transistors

Hana MOBAHI
Universite de Sousse Institut Superieur du Transport et de la Logistique de Sousse
Malek GASSOUMI (malek.gassoumi@gmail.com)
Institut National des Sciences Appliquees de Lyon
MOhamed Ali ZAIDI
Universite de Monastir Faculte des Sciences de Monastir

Research Article

Keywords: AlGaN/GaN/Si HEMTs, impedance spectroscopy, conductance, passivation, electron traps.

Posted Date: April 19th, 2021

DOI: https://doi.org/10.21203/rs.3.rs-391799/v1

Abstract

AlGaN/GaN HEMTs grown on high resistive silicon (111) substrate grown by molecular beam epitaxy have been investigated using impedance measurements. Passivation of the HEMT devices is made in order to improve the electron transport. As has been found from conductance data, the electron traps are eliminated after passivation. The impedance spectroscopy has been, on the other hand, studied from the electrical transport. As a result, a complex impedance plot was revealed an equivalent circuit models indicating single semicircles and the solid interface.

1. Related Works

AlGaN/GaN high electron mobility transistors (HEMTs) are promising candidates for high frequency and high-power applications [1–5]. The main reason is that nitride based materials have large breakdown bias voltages, wide band gaps, efficient carrier transport and extraordinary saturation velocity as well as a low power consumption [6, 7]. As a result, from the strong spontaneous and piezoelectric polarization fields and large conduction band discontinuity, a two-dimensional electron gas (2DEG) can create at the AlGaN/GaN interface with a relatively high electron mobility and high density [8, 9]. The optimization of growth conditions and design parameters improvements the performance of AlGaN heterostructure transistors. However, the AlGaN/GaN HEMTs occasionally exhibit poor reliability leading to a limitation of the devices' performance. For instance, defects, impurities, current collapse, gate-lag and drain-lag will seriously affect the devices' performance and reliability [10–13]. In particular, different techniques have been used to study the origin of the active traps and especially their locations [14–16]. On the other hand, the direct current and the radio-frequency characteristics characterized current collapse, gate-lag and drain-lag. In addition, these phenomena can lead to a degradation in performance for AlGaN/GaN HEMTs operating at large signal conditions. To limitation of the trapping effects and overcome inconveniences for AlGaN/GaN HEMTs as a solution is recommended Surface passivation [8]. As can be noticed, current collapse, gate-lag and drain-lag are reduced by surface passivation [8, 17]. In the present work reports on a study of unpassivated and passivated AlGaN/GaN/Si HEMTs using impedance spectroscopy. For the same HEMT structures, we have also investigated the frequency dependent conductance analysis and the electrical equivalent circuit characteristics.

2. Experiments

The AlGaN/GaN HEMTs under investigation are grown on silicon (111) substrate by using molecular beam epitaxy (MBE). The active layers consist in a 500 nm thick of undoped AlN/AlGaN buffer, a 1.8 μm undoped GaN channel, a 23 nm thick of undoped $Al_{0.26}Ga_{0.74}N$ barrier and a 1 nm n^+- GaN cap layer. The ohmic contact pads are patterned using e-beam lithography. Hereafter, the metallization by means of evaporated 12/200/40/100 nm Ti/Al/Ni/Au is deposited at 900°C during 30s. The Schottky gate is realized using 100/150 nm Mo/Au layers. On the other hand, the AlGaN/GaN/Si HEMTs are passivated by 100/50 nm SiO_2/SiN with N_2O pretreatment. Impedance spectroscopy has been used as a technique to investigate the charge carrier transport mechanisms and relaxation processes in the AlGaN/GaN/Si

HEMTs heterostructures. Measurements were performed using a HP 4192 ALF impedance analyzer at atmospheric pressure and room temperature. Real Z’ and imaginary Z” parts of impedance characterization of the devices are carried out by capacitance and conductance measurements.

3. Conductance Characteristics

The frequency dependent (100 Hz – 10 MHz) conductance measurements is employed to investigate defects in the device. Figure 1 shows the conductance/ω as a function of radial frequency at different bias voltage V_{gs}. It is found that the conductance increases in passivated HEMTs going from 4.10^{-10} to 8.10^{-6} F. As also shown, conductance decreases with frequency at higher range and increases in lower frequency. The conductance signal of an unpassivated AlGaN/GaN/Si HEMT, however, indicates that one deep electron trap is present in the devices. The electron trap could be a defect located at the AlGaN/GaN heterointerface [8, 17, 18]. In addition, this electron trap is related to surface states [8]. As can be noticed, the passivation with N_2O pretreatment led to suppression of traps in surface [8].

4. Impedance Measurements

Impedance spectroscopy has been proven to be a useful tool to understand the interface processes and the transport mechanisms in devices’. Then, we have used this technique to understand the charge transport and study the conductance mechanism in the AlGaN/GaN/Si HEMTs. At an applied frequency, the complex impedance of a system can be written as [19] :

$$Z = Z_R + j\, Z_i = Z' + j\, Z'' \qquad (1)$$

where Z’ and Z” are real and imaginary part components of the impedance. Fig.2 shows the real part of impedance as a function of radial frequency at different bias voltage. As can be seen, the magnitude of Z’ decreases with the frequency increase. On the other hand, the real part of passivated AlGaN/GaN HEMTs shows the presence of constant region and a decreasing tendency at high frequency. In addition, the values of the real part of impedance decreases after passivation with N_2O pretreatment. This means that the quality of the Schottky contact is improved by passivation, however, the decrease in barrier height [8]. Fig.3 shows the imaginary part of impedance signal as a function of radial frequency at different bias voltages. As can be noticed, the spectrum of an unpassivated and passivated AlGaN/GaN/Si HEMTs is composed of one overlapped peak. The variation of the imaginary part of impedance as a function of radial frequency presents a maximum peak at particular frequencies. It is found that the imaginary part of the impedance increases with the radial frequency and reaches a maximum value before decreasing again. In addition, the peak position shifts to higher frequencies and the peak intensity decreases with decreasing bias voltages. This indicates a relaxation time process. It should be noted that the contribution of relaxation process may possibly be explained by the presence of defects in AlGaN/GaN heterointerface. Fig.4 shows the complex impedance plot of an unpassivated and passivated AlGaN/GaN/Si HEMTs at different bias voltages. It is worth noticing that the single semi-circle in complex plane is derived from the ac reponse with frequency. In addition, all the semicircles exhibit some

depression instead of a semicircle centered on the x-axis. It is found that the impedance spectrum is displayed a single semi-circle at bias voltages and the diameter of the semi-circle decreases with decreasing applied bias voltages. It should be noted that the impedance results were analyzed by the Z view Software [20]. However, all spectra could excellently be fitted to the equivalent circuit. Fig.5 shows the complex impedance spectrum at V_{gs} = 0V and the equivalent electrical circuit. This clearly shows that the best fit for the impedance data consisting of an additional series resistance R_s connected in series with two parallel circuits CPE_b/R_b and CPE_t/R_{2DEG}. The impedance of the equivalent circuit at the AlGaN/GaN heterointerface can be expressed as [19] :

$$Z = Z_R + j\,Z_i = R_s + \frac{1}{\frac{1}{R_b} + (2\,j\,f_{ac})^{\alpha_b}.Q_b} + \frac{1}{\frac{1}{R_{2DEG}} + (2\,j\,f_{ac})^{\alpha_t}.Q_t} \quad (2)$$

where R_s, R_b and R_{2DEG} are the resistance of the ohmic contact, cap/barrier layers and 2DEG respectively. CPE_b is the capacitive element of the barrier/cap layer, Q_b is the charge of the barrier/cap layer, CPE_t is the frequency dependent trapping of 2DEG charge carriers and Q_t is the charge of 2DEG. Let CPE be the constant phase element, it is given according to [19] :

$$Z_{CPE} = \frac{1}{(j\,\omega)^{\alpha}\,.\,Q} = \frac{1}{(2\,\pi\,f)^{\alpha}\,.\,Q} \quad (3)$$

with $0 \leq \alpha \leq 1$. For $\alpha = 0$, the system is described by a resistor, while for $\alpha = 1$ an ideal capacitor is described.

It can be noticed that the CPE behavior include varing thickness or composition, surface roughness, or non-uniform current distribution [21-23]. The CPE accounts is used to successfully model an equivalent circuit of AlGaN/GaN heterointerface including effects due to traps and 2DEG depletion and frequency dispersion. The parameters obtained for the electrical equivalent circuit are summarized in Table 1. As can be seen, the resistance (R_s, R_b and R_{2DEG}) decreases after passivation. However, the CPE_t and CPE_b increases due to the defect levels in the AlGaN/GaN HEMTs which create a distribution of charge generation/recombination time constants [19]. It should be noted that the passivation gives rise to a more improved electron transport. This improvement is assigned to the reduction of electron traps.

5. Summary

In the present work, we have investigated the effects of passivation on the transport characteristics of AlGaN/GaN/Si HEMTs. The electrical behavior of the transistor device is characterized by using impedance measurements. As has been shown, passivation of SiO_2/SiN with N_2O pretreatment improves the electron transport and reduces the electron traps. As a consequence, an equivalent circuit model is found to be the best model of correlation electrical properties of the AlGaN/GaN/Si HEMT devices.

Declarations

Author Contributions: All the authors contributed in each part of the

manuscript including framing, and writing the manuscript.

Data Availability: All data included in this paper are available upon request by contact with the contact corresponding author.

Declarations: The authors declare that they have no known competing financial interests or personal relationships that could have appeared to influence the work reported in this paper.

Conflict of Interest: The authors declare that there is no conflict of interest

Consent to Participate All the authors voluntarily agree to participate in

this research study.

Consent to Publication All the authors provide their consent to publish

the present work in the Silicon journal.

Human and Animal Rights This article does not contain any studies

involving animals or human participants performed by any of the authors.

References

1. U.K. Mishra, P. Parikh and Y. F. Wu, Proc. IEEE. 90 (2002) 1022.
2. J.S. Moon, R. Grabar, Brown, IEEE Electron Device Lett. 37 (2016) 272.
3. Y. Pei, Z. Chen, D. Brown, S. Keller, S.P. Denbaars, U. K. Mishra, IEEE Electron Device Lett. 30 (2009) 4.
4. V.Kumar, A. Kuliev, R. Schwindt, M. Muir, G. Simin, J. Yang, M.A. Khan, I. Adesida, Solid-State Electron. 47 (2003) 1577.
5. M.J. Manfra, N. Weimann, Y. Baeyens, P. Roux, D.M. Tennant, Electron. Lett. 39 (2003) 694.
6. H. Morkoç, Handbook of Nitride Semiconductors and Devices, vol. I-III, Wiley-VCH, Berlin,2008.
7. G. Meneghesso, G. Verzellesi, F. Danesin, F. Rampazzo, F. Zanon, A. Tazzoli, M. Meneghini, E. Zanoni, IEEE Trans. Device Mater. Reliab. 8 (2008) 332.
8. H. Mosbahi, M. Gassoumi, I. Saidi, H. Mejri, C. Gaquière, M.A. Zaidi, H. Maaref, Current Applied Physics. 13 (2013) 1359.
9. K. S. Im, J. Choi, Y. Hwang, S.J. An, J. S. Roh, S. H. Kang, J. H. Lee, J. H. Lee, Microelectronic Engineering. 215 (2019) 110985.
10. R. Vetury, N.Q. Zhang, S. Keller, U.K. Mishra, IEEE Trans. Electron Devices. 48 (2001) 560.
11. Y.R. Wu, J. Singh, J. Appl. Phys. 101 (2007) 113712.
12. C. Rivera, E. Muñoz, Appl. Phys. Lett. 94 (2009) 053501.

13. G. Meneghesso, G. Verzellezi, R. Pierobon, F. Rampazzo, A. Chini, U.K. Mishra, C. Canali, E. Zanoni, IEEE Trans. Electron Devices. 51 (2004) 1554.
14. P.B. Klein, J. Appl. Phys. 92 (2002) 5498.
15. O. Mitrofanov, M. Manfra, N. Weimann, Appl. Phys. Lett. 82 (2002) 4361.
16. A.P. Zhang, L.B. Rowland, E.B. Kaminsky, V. Tilak, J.C. Grande, J. Teetsov, A. Vewiatchikh, L.F. Eastman, J. Electron. Matter. 32 (2003) 338.
17. A. Chakraborty, D. Biswas, Appl. Phys. Lett. 106 (2015) 082112.
18. X.H. Ma, J.J. Zhu, X.Y. Liao, T. Yue, W.W. Chen, Y. Hao, Appl. Phys. Lett. 103 (2013) 033510.
19. M. Donahue, B. Lübbers, M. Kittler, P. Mai, A. Schober, Appl. Phys. Lett. 102 (2013) 141607.
20. D. Johnson, ZView : A Software Program for IES Analysis, Version 2.8, Scribner Associates, Inc., Southern Pines, NC, 2002.
21. K. S. Cole, R. H. Cole, J. Chem. Phys. 9 (1941) 341.
22. J. R. Macdonald, W. R. Kenan, Impedance Spectroscopy : Emphasizing Solid Materials and Systems, Wiley Interscience, New York, 1987.
23. G.J. Brug, A. L. G. Van Den Eeden, M. Sluyters-Rehbach, J. H. Sluyters, J. Electroanal. Chem. 176 (1984) 275.

Tables

Table 1: Fitting parameters of impedance data for AlGaN/GaN/Si HEMT devices before and after passivation at V_{gs} = 0V.

	Rs (Ω)	R_b (Ω)	CPE_b (F)	$α_b$	R_{2DEG} (Ω)	CPE_t (F)	$α_t$
Unpassivated	349.2	$6.31.10^{7}$	$2.44.10^{-12}$	1.05	$3.20.10^{7}$	$7.82.10^{-12}$	0.92
Passivated	345	347.4	$3.89.10^{-8}$	0.78	864.3	$9.56.10^{-11}$	1.03

Figures

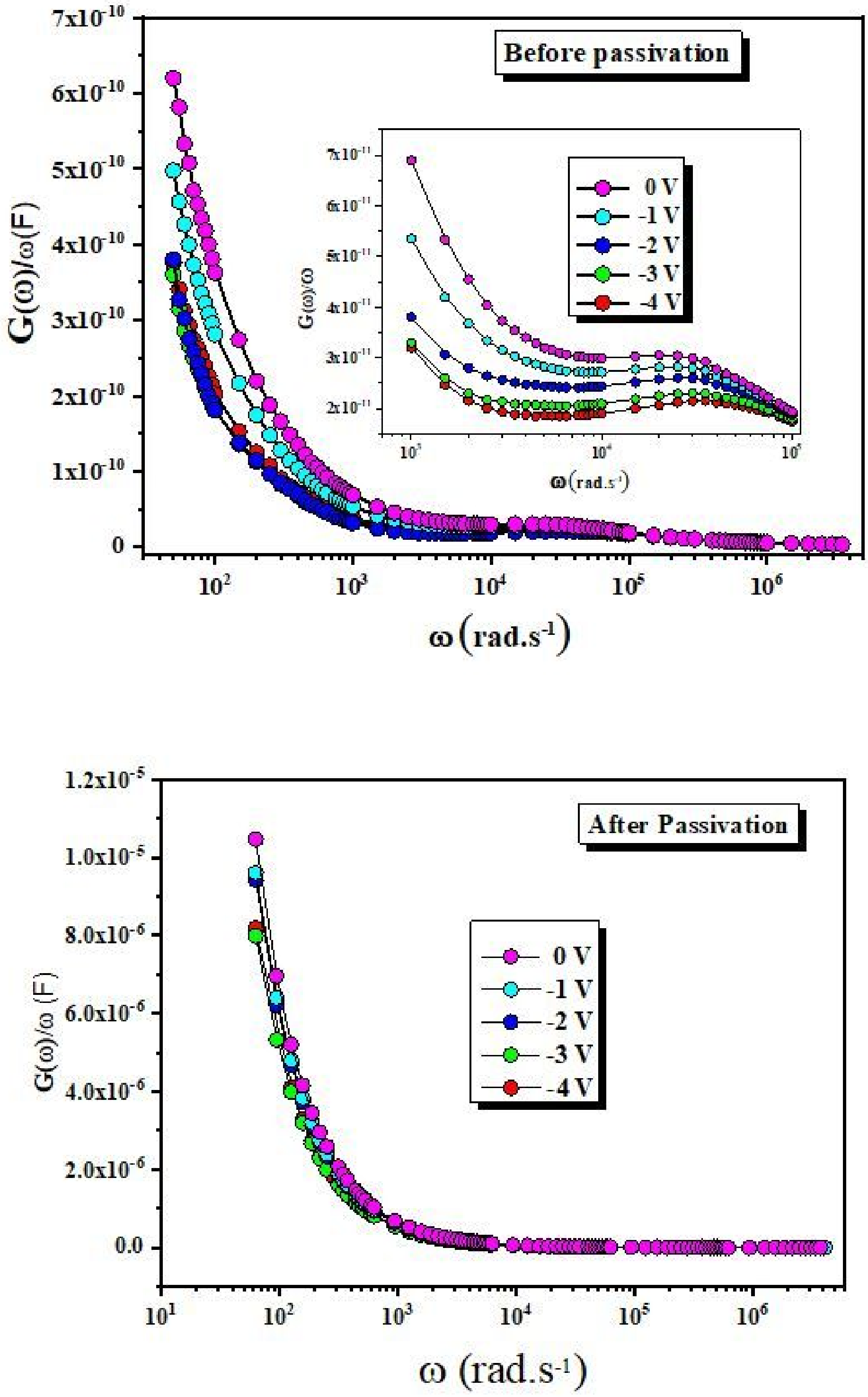

Figure 1

Conductance spectra of the AlGaN/GaN/Si HEMTs.

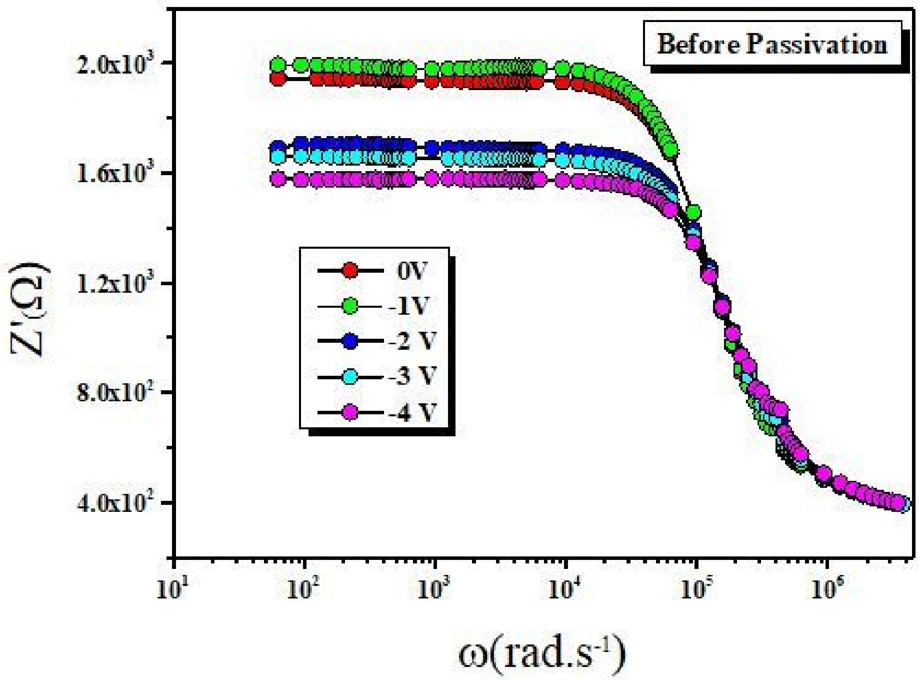

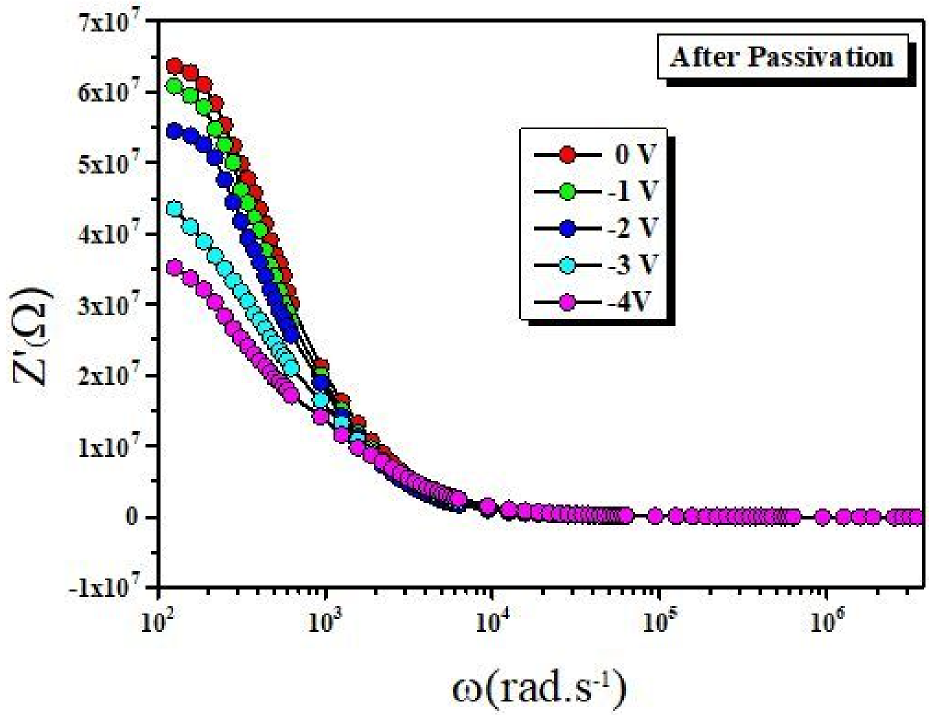

Figure 2

Real part of impedance of the AlGaN/GaN/Si HEMTs at different bias voltage.

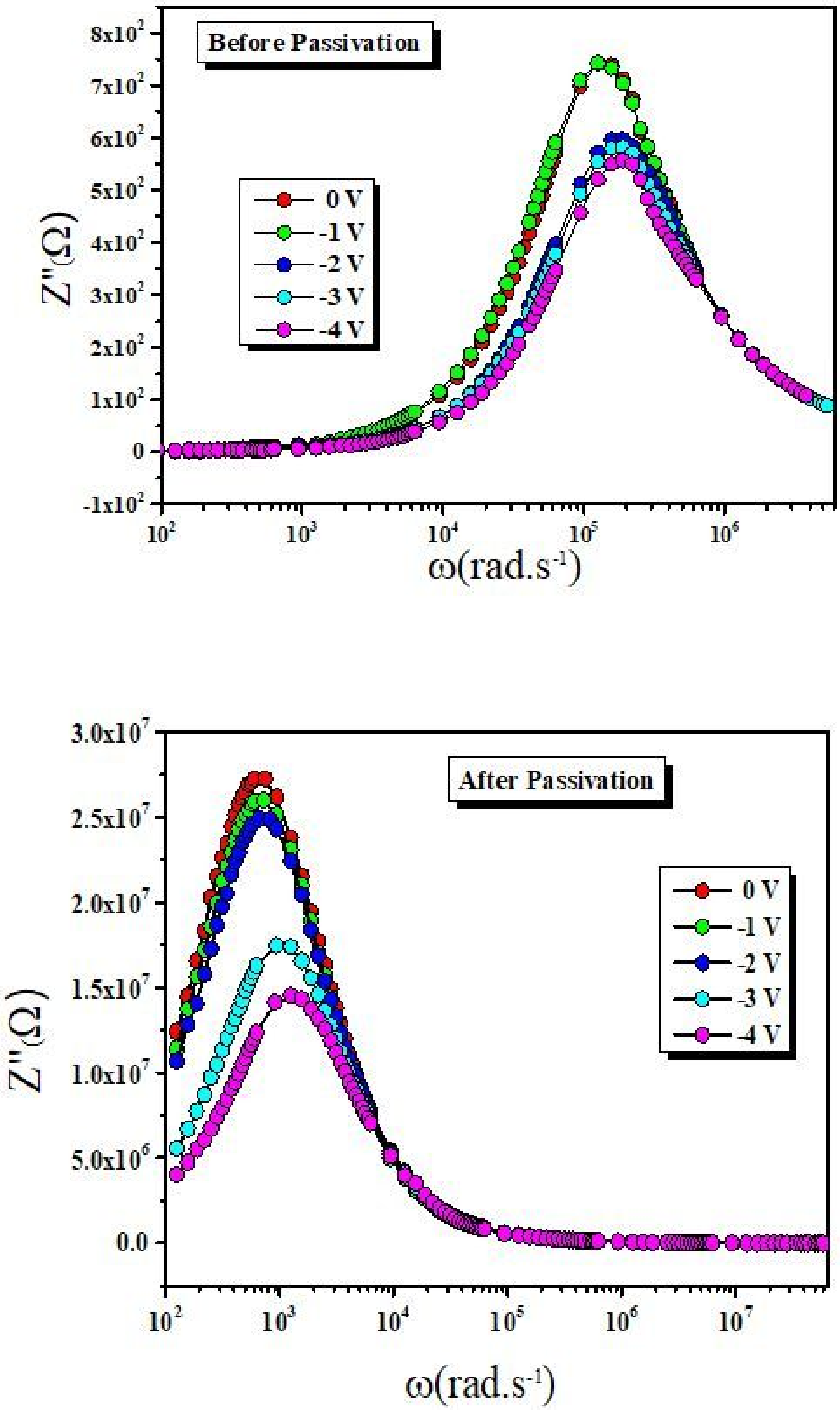

Figure 3

Imaginary part of impedance of the AlGaN/GaN/Si HEMTs at different bias voltage.

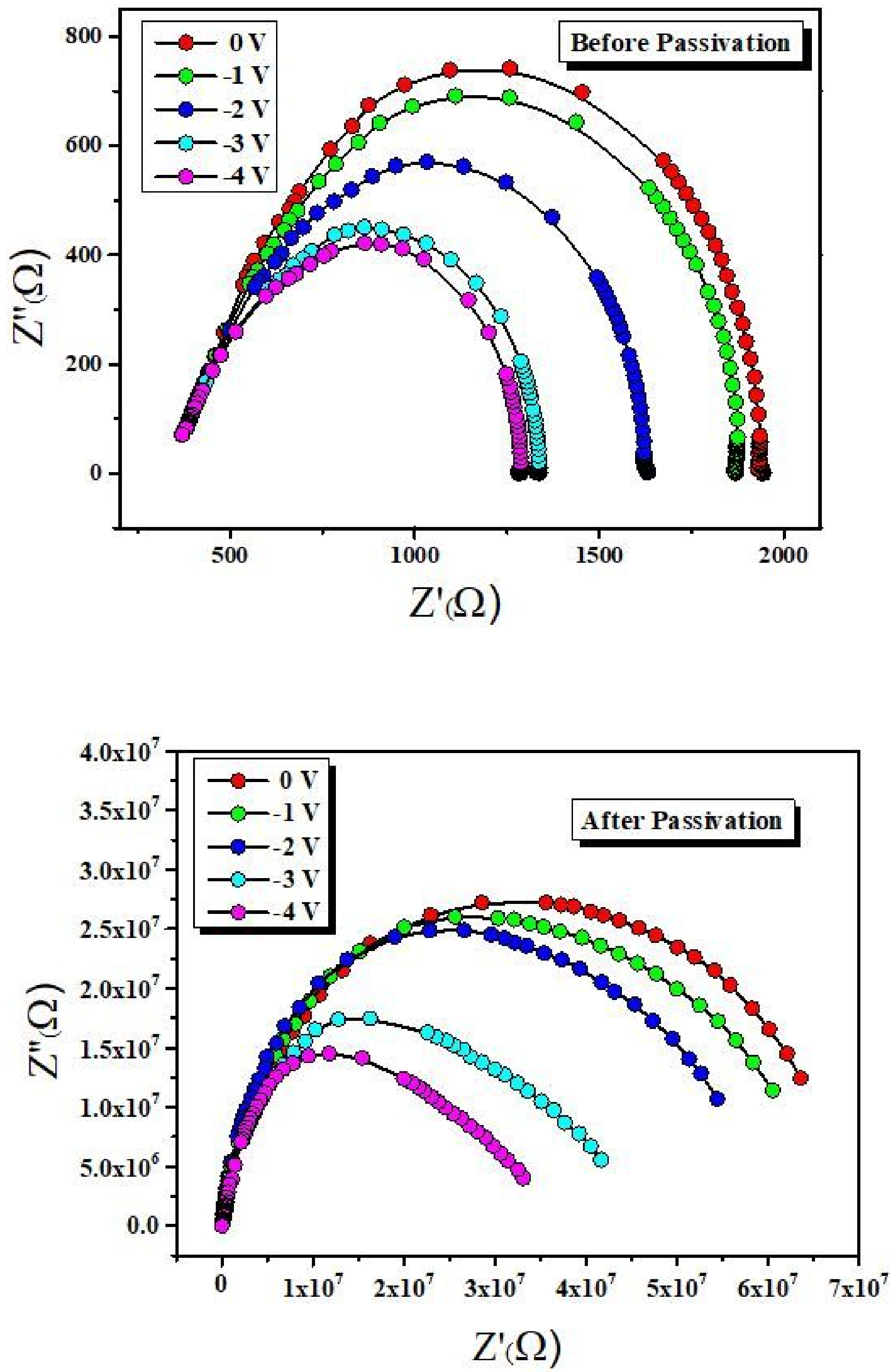

Figure 4

Complex impedance plot of the AlGaN/GaN/Si HEMTs at different bias voltage.

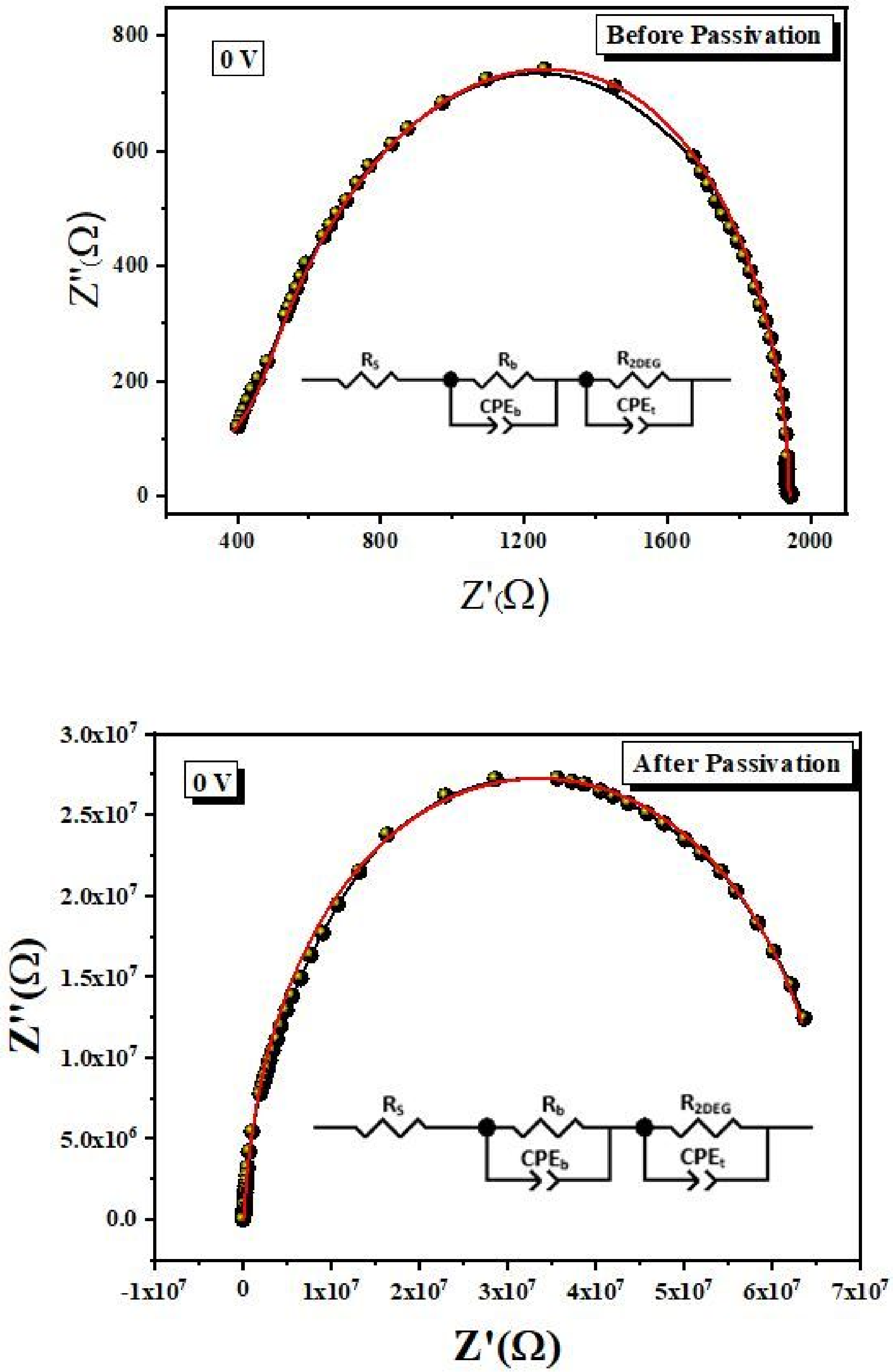

Figure 5

Complex impedance spectrum at Vgs = 0V and the AlGaN/GaN/Si HEMTs equivalent circuit.